New Production Modeled from Nitrate Reductase Activity for the Peru Current Upwelling

S. González-Galisteo[a,*], T. T. Packard[a], M. Gómez[a], A. Herrera[a], R. C. Dugdale[b], F. P. Wilkerson[b], R. T. Barber[c], D. Blasco[d], J. P. Christensen[e], L. A. Codispoti[f]

[a] *Marine Ecophysiology Group (EOMAR), IU-ECOAQUA. Universidad de Las Palmas de Gran Canaria, Canary Islands, Spain.*
[b] *Romberg Tiburon Center, San Francisco State University.*
[c] *Nicholas School of the Environment and Earth Sciences, Duke University.*
[d] *Institut de Ciències del Mar (CSIC).*
[e] *Green Eyes LLC.*
[f] *Horn Point Laboratory, University of Maryland Center for Environmental Science, Cambridge, MD 21613-0775, USA.*

Abstract

We have developed a light-dependent, nitrate and ammonium independent model of new production based on phytoplankton nitrate reductase (NR) activity that predicts strong new production off Peru. The model is based on measurements from the Coastal Upwelling Ecosystem Analysis (CUEA) JASON expedition from September 1976. The new production at the 50% light level in the euphotic zone ranged from 3.49 μM C h^{-1}, 12 km downstream from the upwelling center to 0.15 μM C h^{-1}, 46 km further downstream over the 4000 m deep Peru Trench where the upwelling was relatively weak. It compared well with ^{14}C carbon productivity measurements whose range was 0-4.2 μM C h^{-1} and 0-1.5 μM C h^{-1} for the 6 h (gross) and 24 h (net) produc-

*Corresponding author. Tel.: +34 928 45 44 40; fax: +34 928 45 29 22
Email address: sara.gonzalez115@alu.ulpgc.es (S. González-Galisteo)

tivity, respectively. In nitrogen units, the overall new production ranged from 4 to 510 nM of N h^{-1} . The oceanographic conditions found during September 1976 made this site in the Peruvian upwelling an ideal one to model new production. Temperature in the center of the upwelling in September of 1976 reached 14.07°C, while NO_3^- and NO_2^- ranged from 6.65 to 7.5 and 0.51 to 1.6 μM respectively. Chlorophyll, averaging 3.85 μg L^{-1} for the section stations in September 1976, was similar to what it was for all the stations 6 months later in March 1977 (3.23 μg L^{-1}). NR, averaging 0.20 μM N h^{-1} for the section stations in September 1976, was twice what it was for all stations, 6 month later in March 1977 (0.09 μM N h^{-1}).
Keywords: primary production, nitrogen uptake, nitrate, ammonium, light, phytoplankton.

---

1. Introduction

Nitrogen, although only 16% of the carbon in cells, is still of key importance in the geosphere-biosphere elemental transition. For this reason, the nitrogen uptake rate is an important measure of marine ecosystem productivity (Dugdale and Goering, 1967; MacIsaac and Dugdale, 1969, 1972). Nitrogen (N) can be supplied to phytoplankton independently from three sources, as seen in the N cycle of Fig. 1. One uptake pattern is based on N-fixation and uptake of N oxides, primarily NO_3^-. Production driven by these two processes is known as "New Production" or NP. The second uptake pattern is based on reduced N forms, primarily NH_4^+ and urea, supplied by bacterial remineralization or zooplankton and nekton excretion. Both processes "regenerate" simple nitrogen-rich ions or molecules from proteins or

nucleotides. This type of production is known as "Regenerated Production" or RP (Dugdale and Goering, 1967). This work focuses on modelling nitrate-based "New Production" because it is a major contributor to productivity in marine upwelling ecosystems. In all oceanic ecosystems, new production is the photosynthetic formation of phytoplankton biomass stimulated by nitrate fluxing from subsurface waters into the euphotic zone and by diazotroph-driven nitrogen fixation (Dugdale and Goering, 1967; Dugdale et al., 1992). New production is high in all upwelling areas, in open ocean areas after major turbulent events (storms, winter mixing, etc.) and low in stratified nutrient-poor waters such as central gyres and the Arctic Ocean. Forty-five Pg. yr^{-1} (10^{-15} g yr^{-1}) is a recent estimate of Global Ocean Production by the Oregon state SeaWifs program (www.science.oregonstate.edu/ocean.productivity/). With an f-ratio of 0.25 (New Production /Total Production) this would mean a new production of 11 Pg yr^{-1} (3 Tg (10^{-12} g) h^{-1}), assuming the production occurred in ten daylight hours. New production is measured on bottled phytoplankton samples by the ^{15}N technique (Dugdale et al., 1961; MacIsaac and Dugdale, 1969; Dugdale and Wilkerson, 1998). However, in theory, this NO_3^- uptake can be modeled from nitrate reductase activity, its dependence on nitrate and light, and its control kinetics (Packard et al., 1971). Assimilatory nitrate reduction in algae, plants, bacteria and archaea is catalyzed by nitrate reductase (NR), the enzyme that reduces nitrate (NO_3^-) to nitrite (NO_2^-) (Eq. 1). It is the first step in incorporating N into protein (Fig. 2). Assimilatory NR is not found in protozoans, metazoans, or higher animals (Fig. 3) except under conditions of endosymbiosis (Packard et al., 1978; Collos and Berges, 2003).

$$NO_3^- + NADH + 2e^- + H^+ \rightarrow NO_2^- + NAD^+ + H_2O \quad (1)$$

In marine algae, NR can be found in the plasmalemma and other cellular membranes of diatoms, chlorophytes, and cyanobacteria (Jones and Morel, 1988; Tischner et al., 1989; Berges, 1997; Dagenais-Bellefeuille and Morse, 2013); in dinoflagellates, it can be found in chloroplasts, where most of the NO_3^- reduction takes place (Berges and Mulholland, 2008); and in chlorophytes it can be found in pyrenoids (Glibert et al., 2015). NR operates in conjunction with low affinity nitrate transporters (LANT) the enzymes that are the responsible for the diffusion of environmental NO_3^- into the cell; nitrite reductase (NiR), the enzyme that reduces NO_2^- to ammonium (NH_4^+); and glutamine synthetase (GS), the enzyme that fixes NH_4^+ into glutamate ((COOH)-$(CH_2)_2$-CH(NH_2)-(COOH)), a key precursor in amino acid synthesis (Glibert et al., 2015).

Nevertheless, of all the enzymes that operate in the process, the rate limiting step of the reaction is catalyzed by NR (Beevers and Hageman, 1969; Tischner, 2000; Young et al., 2007). That is why it can be used as a measure (proxy) of N-uptake as well as an estimation of the NO_3^- assimilation rate (Packard et al., 1971; Gordillo et al., 1997; Collos and Berges, 2003). It is a sensitive enzyme because it is light dependent, stimulated by NO_3^- , and inhibited by NH_4^+. In the dark NR is normally inactivated. Also, if NO_3^- is absent or if NH_4^+ is present in seawater, NR is inactivated. In zooplankton-rich seawaters it is repressed by NH_4^+ excretion and deep in a NO_3^- -rich water column by the low light. On the other hand, when NO_3^-

is present and NH_4^+ is absent, NR activity follows an endogenous diel cycle (Eppley et al., 1970; Packard et al., 1971; Young et al., 2007). Because of these characteristics, NR is rarely measurable in the oligotrophic ocean, except during blooms, but it is easily measured in NO_3^- -rich coastal upwelling areas. Given these sensitivities, NR activity should be a useful oceanographic indicator of new production (Hung et al., 2000; Packard et al., 2004), but to date it has not been used as synoptic tool to reveal the new production in an upwelling area. Here, this is done.

We develop a light-dependent, nitrate and ammonium independent model of new production based on NR activity that predicts strong new production off Peru. The model is based on NR measurements from the Coastal Upwelling Ecosystem Analysis (CUEA) JASON expedition from September 1976 (Packard and Jones, 1976) and the conceptual idea from Packard et al. (1971) and Berges and Harrison (1995).

2. Materials and Methods

2.1. Research site

The site of this study was 15°S off Pisco, Peru (Fig. 4a), a zone characterized by a strong and persistent upwelling (Wooster, 1961; Fernández et al., 2009). It was the focus of the Peru phase of the Coastal Upwelling Ecosystem Analysis (CUEA) program of which the JASON-76 expedition was part.

To observe the upwelling variability under such conditions, the JASON-76 expedition took place in the late winter and austral spring (August, Septem-

ber, October and November) when the southeast trade winds intensify to the maximum (Wooster, 1961). The results presented here are from the September 10 to September 22 phase (leg IV) of JASON-76 expedition with the R/V Eastward, cruise no. E-5H-76 (Packard and Jones, 1976).

2.2. Sampling procedures

Seawater samples were taken with Niskin Bottles and with a Rosette Sampler along a transect line (C-Line) (Fig. 4b) across the Peru current at 15°S. The C-Line extended from the coast, at position C-1, across the Peru trench to position C-14, 200 km offshore (Fig. 5). Two hydrosections, multiple productivity, and several deep-biology stations were taken during this cruise. The productivity and deep-biology stations focused on the biological and biochemical properties as well as the nutrient chemistry in the water column. Sampling depths were established according the light; euphotic zone samples were taken at depths where the light was 100, 50, 30, 15, 5, 1 and 0.1% of the surface incident radiation. Four L samples were taken from the morning productivity rosette (Barber et al., 1978), and filtered through 4.25 cm Gelman glass fiber filters (0.7 μm pore size). These samples were assayed for NR activity by nitrite-detection method of Hewitt and Nicholas (1964) as developed for phytoplankton by Eppley et al. (1969) and Packard et al. (1971). The precision of the method was improved by quenching the reaction with Zn acetate before the ethanol, mixing the solution, and then making up to 10 ml. Subsamples were taken for phytoplankton productivity, inorganic nutrients (PO_4^{-3}, NO_3^-, NO_2^- and silicate), ETS activity and protein according to Packard and Jones (1976)

3. Theory and calculations

As said above, new production is the photosynthetic formation of phytoplankton biomass driven by NO_3^- input into the euphotic zone and by N fixation produced by diazotrophic organisms. However, in most coastal upwelling systems, the diazotrophic contribution is practically null compared with the production driven by NO_3^- assimilation, as we see in the N-productivity measurements found in the upwelled and the peripheral water masses off Vietnam in July 2003 and July 2004 (Loick-Wilde et al., 2016). Their study showed, in table 1, that the contribution of N fixation to total primary production (PP) was less than 10% of the PP driven by NO_3^- assimilation, hence, we can neglect, in our study, the diazotroph contribution and consider only the NO_3^- assimilation, measured by the NR activity, as the driver of new production in this area. A similar conclusion can be made from the N-fixation measurements of Fernandez et al. (2011). They calculated a N-fixation of 60 pmol L^{-1} h^{-1} for the Peru-Chile upwelling, where pmol signifies 10^{-12} moles of N. The N (regenerated) productivity for this region at the same time was 6.3 nmol L^{-1} h^{-1}, a hundred-fold larger than the N-fixation (Fernández et al., 2009). The new production at that time was lower than the regenerated production because the NH_4^+ regeneration rates were high (2.8 nmol NH_4^+ L^{-1} h^{-1}). This simplifies the model presented below.

3.1. Modeling New Production

The new production model was based on: (1) the knowledge that NR regulates the first step in the phytoplankton NO_3^- assimilation processes; (2)

the assumption that nitrogen fixation, here, by the diazotrophs is negligible; (3) that a measurement of NR activity yields the V_{max}, the potential or the capacity of the enzyme reaction to reduce NO_3^- to NO_2^- (Eq.2); (4) the dependence of NO_3^- uptake and NR activity on light and $[NO_3^-]$ (MacIsaac and Dugdale, 1969; Packard, 1973; Packard et al., 1978), (5) the inverse dependence of NR on $[NH_4^+]$ (Packard et al., 1971; Packard and Blasco, 1974; Glibert et al., 2015) and (6) that the $[NH_4^+]$ in the euphotic zone off 15°S was too low to inhibit NR.

$$V = \frac{V_{max}[S]}{K_m + [S]} \tag{2}$$

In ocean waters charged with ample NO_3^-, and relatively low NH_4^+ the model can be expressed as a light-dependent, single substrate Michaelis-Menten equation (Eq. 3):

$$New\ Production = \frac{NR \cdot [light]}{K_m + [light]} \tag{3}$$

Here, NR represents the V_{max} of the NR-catalysed NO_3^- reduction reaction, expressed in μM h^{-1}. [Light] is the light level as a % of surface radiation, here expressed either in Langleys (ly) min^{-1} or % of surface radiation ($\%I_0$) (Martinez et al., 1987), but for equation 4 we used $\%I_0$. The K_m which we referred to as the "light-K" (K_{LT}), is the NR Michaelis-Menten constant for light. The calculated new production is expressed in μM h^{-1}, the same units as the NR.

The measurements show that in the euphotic zone NO_3^- along the C-Line was always above 6 μM (Fig. 7a), and that the NH_4^+ was always below 0.1 μM. These conditions support the simplification of the enzyme kinetics to a single substrate case based on light. Accordingly, we can write Eq. 3 for the New Production Rate (NPR) as a differential equation (Eq. 4):

$$NPR = -\frac{[\partial NO_3^-]}{\partial t} = -\frac{[NR] \cdot [h_v]}{K_{LT} + [h_v]} \tag{4}$$

Where [NR] is, again, the V_{max} of the NO_3^- reduction reaction, expressed in μM h^{-1}. [h_v] is [light] expressed in $\%I_0$, and K_{LT} is 2.4% I_0, taken from a previous upwelling study (Table 2 in Martinez et al. (1987)). Resulting NPR is expressed in μM h^{-1}. sectionResults

3.2. Oceanographic conditions

Off Peru, low sea surface temperatures usually indicate upwelling intensity (Dugdale, 1972). In September 1976, classified as an ENSO transition year (Santoso et al., 2014), it was observed that the upwelling was more intense than in previous months. Sea surface temperatures at C-3, the center of the upwelling were usually low. In September 1976 they averaged 14.07°C (Fig. 6a), more than 2 degrees lower than they were in the following fall season and 1 degree lower than they were in spring (August-September) 10 years later (Minas et al., 1990). From 28 March to 8 April 1977 the average temperature was 16.65°C (Packard et al., 1978) and during the French Paciprod cruise of the R/V Jean Charcot in August-September 1986 it dropped only

to 15°C in the same upwelling center (Dugdale et al., 1995). The surface σ_t between C-1 and C-3 was below 26.0 (Fig. 6b), evidence that the surface water in these upwelled waters rose from depths below 100 meters, at C-14 (Packard et al., 2015). From a study of the same C-Line section made during the 1986 Paciprod cruise in the same season of the year, Dugdale et al. (1995) found that the upwelled waters at C-3 were originated at 120 meters in the vicinity of C-14. Large and dense populations of diatoms, most belonging to the group Chaetoceros, were found in the first meters of the water column, in the euphotic zone (Rojas de Mendiola, 1976), especially at C-3.

3.3. Productivity stations

Following the description in the methodology, productivity and biochemical measurements are presented in (Table 1). In September 1976, NO_3^- ranged from 6.65 to 17.5 μM throughout the euphotic zone from C-1 to C-12. It never fell below 6.65 μM. The maximum (15.24 μM) occurred at the sea surface (0 m) in the upwelling center, C-3. At the bottom of the euphotic zone, at C-3 (Sta 21), NO_3^- reached a high of 17.5 μM (Table 2 and Fig. 7a). The lower values of NO_3^- at C-5 and C-12 reflected biological uptake (Fig. 7a). The NO_2^- section (Fig. 7b) had two subsurface maxima (1.1 μM) at the bottom of the euphotic zone. The first (1.13 μM) occurred at C-1, near the coast, and extended vertically all the way to the surface. The second was a NO_2^- patch spreading horizontally from C-Line positions C-5 to C-8, between 21 and 29 m (Table 2 and Fig. 7b). A third subsurface maximum of 1.6 μM occurred at 20 m at C-Line position C-12; this one coincided with a NO_3^- minimum zone in the waters above. Overall, the NO_2^- concentrations in the euphotic zone ranged from 0.51 to 1.6 μM, with

a water column minimum at C-10 (Fig. 7b). Chlorophyll section revealed two maxima, the first one at C-5 and the second one at C-12 (Fig. 8a). Both rose to 8 mg m^{-3}. The first was displaced offshore by about 10 km from the silicate and NO_3^- maxima at the upwelling center (Figs. 8b and 7a); the second coincided with a silicate and NO_3^- minimum (Figs. 8b and 7a) and extended down to 40 m in the water column. Ten years later on the Paciprod cruise chlorophyll concentrations were much lower, between 20% to 50% of the JASON-76 chlorophyll. In addition, the chlorophyll maximum in 1986 was displaced about 30 km offshore from its position at C-5 in 1976 (Fig. 8a). As for the silicate section (Fig. 8b), it was high over the shelf in the upwelling area, ranging from 21.7 to 27.2 μM (from C-1 to C-3) and low seaward of the Peru Trench, averaging around 7.3 μM (from C-10 to C-12)(Fig. 8b). The high levels of silicate in the upwelling center were about twice what Dugdale et al. (1995) reports from the Paciprod cruise at the same place in spring 1986. However, offshore the nitrate and silicate return to their normal 1:1 ratio (Dugdale et al., 1995). The decrease is an indication of diatom uptake (Dugdale and Wilkerson, 1998), but with the silicate nearly twice the nitrate in the upwelling center it is unlikely to be controlling new production as Dugdale et al. (1995) found from modeling this ecosystem 10 years later.

The carbon productivity (^{14}C) distributions are shown in Fig. 9 (a and b). Measurements reveal highest values in the near-surface water for both the 6 and 24 hours incubation bottles. Overall, the two productivity measurements ranged from 0 to 4.2 and 0 to 1.5 μM of carbon per hour, respectively. Here, we interpret the 6 h C-productivity as gross or total productivity and

the 24 h C-productivity as net productivity. Using the Redfield C:N ratio of 6.6 (Geider and La Roche, 2002) these ranges become 0 to 0.64 and 0 to 0.23 μM N h^{-1}. Both correlate with the NR as expected if new production is related to carbon productivity.

The new production model, the NR measurements and the light intensity measurements in both ly min^{-1} and $\%I_0$ are presented in Table 2. Nitrate reductase (NR) was measured in the euphotic zone throughout the water column at all stations (Tables 1 and 2). It ranged from 0 to 0.56 μM h^{-1} in September 1976 (Fig. 10), lower than NR measured in March 1977 which ranged from 0 to 0.92 μM h^{-1}. Here, in contrast to the mesopelagic (subsurface) bacterial NR measurements made along the C-Line in fall, 1977 (Packard et al., 1978), special attention was paid to the phytoplankton in the light-rich surface waters where nitrate was plentiful and NR activity was extraordinary high. The NR vertical distribution revealed high values near the surface, where light is unlimited. Two maxima appear, the first and most intense one was at C-5; the second occurred at C-12 (Fig. 10). Both coincided with new production maxima calculated according Eq. 4 and represented in Table 2, Fig. 11a and b. From Table 2 the new production ranged from 4 to 550 nM N h^{-1} (0.03 to 3.61 μM C h^{-1}) along the C-Line in September 1976. During the same season 10 years later (1986) the new production, modeled from nutrient and hydrographic measurements and a new concept of silicate limitation of diatom growth, ranged from 5 to 10 nM N h^{-1}. The model also found that, at that time, ammonium-based regenerated production ranged from 7.5 to 2.5 nM N h^{-1}. In our study in 1976 the ammonium levels were low

and from Fig. 13a the total productivity was composed entirely of new production. Otherwise the slope of Fig. 13a would have been much lower than 0.96. In any case the NR-based model predicted a two-order of magnitude range of new production for 1976.

4. Discussion

From our previous research (MacIsaac and Dugdale, 1969; Eppley et al., 1970; Packard et al., 1971; Blasco and Packard, 1974; Dugdale, 1985; MacIsaac et al., 1985; Martinez et al., 1987), we knew that NR activity was enhanced by light; followed a diel cycle; was stimulated by nitrate; and was inhibited by NH_4^+. Glibert et al. (2015) confirms these properties of NR. We also knew that the production off Peru is driven by the vertical flux of inorganic nutrients, especially nitrate. Since phytoplankton NO_3^- assimilation is the main component of new production (Dugdale and Goering, 1967; Dugdale, 1985) and since NR controls it, NR should serve as a measure for potential new production. Packard et al. (1971) hypothesized that nitrate uptake (RNO_3^-) would be a linear function of NR, related to NR by a constant (C) so that RNO_3^- would equal C [NR]. Blasco et al. (1984) showed this to be true, but also showed that the linear relation was clouded by high variability. Here, we make an attempt to explore the use of Michaelis-Menten kinetics (Eqs. 3 and 4) to reduce this variability to improve the prediction of RNO_3^-. New production by the ^{15}N method was not made on this cruise, so the new production prediction from NR can only be verified by its relationship with the 6h ^{14}C productivity measurements. This is done in Fig. 13a. The results argues that new production and gross production are effectively equal and that

regenerated production played an insignificant role in this part of the Peru upwelling in September 1976. Table 3 shows that new production ranged from 0.69 to 6.39 mmol N m^{-2} h^{-1}. About 10 km downstream between C-4 and C-5, just over the shelf edge occurs the new production maximum at 6.39 mmol N m^{-2} h^{-1}. Further offshore over 2000 m of ocean, in the middle of the eastern wall of the Peru trench, the new production was at its minimum, 0.69 mmol N m^{-2} h^{-1}. Further offshore (90 km), perhaps in response to Ekman pumping in response to the curls of the wind stress (Pickett and Paduan, 2003) the new production rises to 4.49 mmol N m^{-2} h^{-1} at C-12 (Table 3, Fig. 11). It is interesting that the global total new production (Duce et al., 2008), normalized by the ocean's surface ($357 \cdot 10^6$ km^2) is 0.044 mmol N m^{-2} h^{-1}, about two orders of magnitude lower than our calculations for the Peru upwelling. This is to be expected because most of the world's oceans are oligotrophic with negligible new production.

Since phytoplankton nitrogen metabolism is responsible for NR activity in the euphotic zone, NR should be correlated with chlorophyll, but except for Eppley et al. (1969) and Eppley et al. (1970) the literature is not strong on this topic. We checked this relatonship with the integrated data in Table 3. Fig. 12 shows a relationship that is described by the equation NR=0.049-0.273 (r^2=0.67, n=6). This means that the NR/Chl ratio is 49 μmol NO_3^- reduced per μg Chl a. Eppley et al. (1970) report 35 μmol NO_3^- reduced per μg Chl a. for the same location in the Peruvian upwelling in 1969.

Although carbon fixation is composed of both new and regenerated pro-

duction, if the NH_4^+ levels are low, as during JASON-76, then new production should correlate with carbon productivity (Eppley and Peterson, 1979) Fig. 13 shows that, in spite of the scatter, this holds true for both our 6h-based and our 24h-based ^{14}C productivity data. The former likely represents gross production. The fact that a ^{14}C determined-gross productivity versus an NR-derived new production calculation has a 1:1 relationship, argues for new production dominance, negligible regenerated productivity, and f-ratio of nearly 1 (Eppley and Peterson, 1979).

5. Conclusions

The model developed here calculates realistic levels of new production, but will need future comparison with new production measured by the ^{15}N technique. The main conclusions of this work are set forth below.

Modeled new production ranging between 0.004 and 0.55 μM of N h^{-1}, (0.03-3.61 μM C h^{-1}) here, has the same distribution pattern as the ^{14}C-based primary production (Figs. 9, 11 and 13). The ^{14}C (24h) and ^{14}C (6h), representing net and gross productivity respectively, ranged between 0-1.5 and 0-4.2 μM C h^{-1}.

New production was highest 12 km downstream of the upwelling center and 25 km upstream of where there co-occured a maximum in the water column respiration, carbon flux and heterotrophic energy production, and a minimum in the nutrient retention efficiency and benthic respiration (Packard et al., 2015). This was at the CUEA C-Line positions C-5, a position over

the upper part of the continental slope.

Temperature and density (σ_t) across the Peru shelf at 15°S, in September 1976, clearly evidenced upwelling. Temperatures as low as 14.07°C and density (σ_t) as high as 26.0 were found in the upwelling center at C-3. The temperature was more than 2°C lower than in March 1977 (16.65°C).

NO_3^- and NO_2^- over the Peruvian shelf and trench ranged between 6.65 to 17.5 μM and 0.51 to 1.6 μM respectively, making this section an ideal research site to study and model new production.

Chlorophyll averaged for all the stations was 3.85 μg L^{-1} slightly higher than it was in March 1977 (3.23 μg L^{-1}). NR averaged 0.21 μM N h^{-1} for the cross-shelf section on 16-22 September 1976. This was twice what it was for all stations in March 1977 (0.09 μM N h^{-1}).

Acknowledgements

We thank J. Ammerman, N. Coble and J. Kogelschatz for help with the cruise. NSF (USA) grant OCE 75-23718A01 (TTP) funded JASON-76. S. G-G. was self-funded. T.T.P. was largely supported by TIAA-CREF and Social Security (USA), but also partially by the Canary Islands CEI: Tricontinental Atlantic Campus. This work was completed while S.G.-G. was a student in the ULPGC Graduate Program in Oceanography.

6. References

Barber, R.T., Huntsman, S., Kogelschatz, J., Smith, W., Jones, B., 1978. Coastal Upwelling Ecosystems Analysis. Data Report 49. Carbon, Chlorophyll and Light Extinction from JOINT II. CUEA Data Report. Technical Report. Bigelow Laboratory for Ocean Sciences.

Beevers, L., Hageman, R.H., 1969. Nitrate reduction in higher plants. Annual Review of Plant Physiology 20, 495–522.

Berges, J.A., 1997. Miniview : Algal nitrate reductases. Eur. J. Phycol 32, 3–8.

Berges, J.A., Harrison, P.J., 1995. Nitrate reductase activity quantitatively predicts the rate of nitrate incorporation under steady state light limitation: A revised assay and characterization of the enzyme in three species of marine phytoplankton. Limnology and Oceanography 40, 82–93.

Berges, J.A., Mulholland, M.R., 2008. Enzymes and Nitrogen Cycling.

Blasco, D., Macisaac, J.J., Packard, T.T., Dugdale, R.C., Hancock, A., Angeles, L., 1984. Relationship between nitrate reductase and nitrate uptake in phytoplankton in the Peru upwelling region. Limnology and Oceanography 29, 275–286.

Blasco, T., Packard, T., 1974. Nitrate reductase measurements in upwelling regions: Baja California and Northwest Africa. I. Significance of the distribution. Tethys 6, 239–246.

Collos, Y., Berges, J.A., 2003. Nitrogen Metabolism in Phytoplankton, in: Marine Ecology: Encyclopedia of Life Support Systems (EOLSS). Eolss Publishers, Oxford, UK, pp. 262–280.

Dagenais-Bellefeuille, S., Morse, D., 2013. Putting the N in dinoflagellates. Frontiers in Microbiology 4, 369.

Duce, R.A., LaRoche, J., Altieri, K., Arrigo, K., Baker, A.R., Capone, D.G., Cornell, S., Dentener, F., Galloway, J., Ganeshram, R.S., Geider, R.J., Jickells, T., Kuypers, M.M., Langlois, R., Liss, P.S., Liu, S.M., Middelburg, J.J., Moore, C.M., Nickovic, S., Oschlies, A., Pedersen, T., Prospero, J., Schlitzer, R., Seitzinger, S., Sorensen, L.L., Uematsu, M., Ulloa, O., Voss, M., Ward, B., Zamora, L., 2008. Impacts of atmospheric anthropogenic nitrogen on the open ocean. Science 320, 893–897.

Dugdale, R., Wilkerson, F., Minas, H., 1995. The role of a silicate pump in driving new production. Deep Sea Research Part I: Oceanographic Research Papers 42, 697–719.

Dugdale, R.C., 1972. Chemical Oceanography and Primary Productivity. Geoforum 3, 47–61.

Dugdale, R.C., 1985. The effects of varying nutrient concentration on biological production in upwelling regions. California Cooperative Oceanic Fisheries Investigations 26, 93–96.

Dugdale, R.C., Goering, J.J., 1967. Uptake of new and regenerated forms of nitrogen in primary productivity. Limnology and Oceanography 12, 196–206.

Dugdale, R.C., Menzel, D.W., Ryther, J.H., 1961. Nitrogen fixation in the Sargasso Sea. Deep Sea Research 7, 297–300.

Dugdale, R.C., Wilkerson, F.P., 1998. Silicate regulation of new production in the equatorial Pacific upwelling. Nature 391, 270–273.

Dugdale, R.C., Wilkerson, F.P., Barber, R.T., Chavez, F.P., 1992. Estimating New Production in the Equatorial Pacific Ocean at 150øW. Journal of Geophysical Research 97, 681–686.

Eppley, R.W., Packard, T.T., MacIsaac, J.J., 1970. Nitrate reductase in Peru current phytoplankton. Marine Biology 6, 195–199.

Eppley, R.W., Peterson, B.J., 1979. Particulate organic matter flux and planktonic new production in the deep ocean. Nature 282, 677–680.

Eppley, R.W., Rogers, J.N., Mccarthy, J.J., 1969. Half-saturation constants for uptake of nitrate and ammonium by marine phytoplankton. Limnology and Oceanography 14, 912–920.

Fernández, C., Farías, L., Alcaman, M.E., 2009. Primary production and nitrogen regeneration processes in surface waters of the Peruvian upwelling system. Progress in Oceanography 83, 159–168.

Fernandez, C., Farías, L., Ulloa, O., 2011. Nitrogen fixation in denitrified marine waters. PLoS ONE 6, 1–9.

Geider, R., La Roche, J., 2002. Redfield revisited: variability of C:N:P in marine microalgae and its biochemical basis. European Journal of Phycology 37, 1–17.

Glibert, P.M., Wilkerson, F.P., Dugdale, R.C., Raven, J.A., Dupont, C.L., Leavitt, P.R., Parker, A.E., Burkholder, J.M., Kana, T.M., 2015. Pluses and minuses of ammonium and nitrate uptake and assimilation by phytoplankton and implications for productivity and community composition, with emphasis on nitrogen-enriched conditions. Limnology and Oceanography 61, 165–197.

Gordillo, F.J.L., Jiménez, C., Corzo, A., Niell, F.X., 1997. Optimized nitrate reductase assay predicts the rate of nitrate utilization in the halotolerant microalga Dunaliella viridis. Journal of Applied Phycology 9, 99–106.

Hewitt, E.J., Nicholas, D.J., 1964. Enzymes of inorganic nitrogen metabolism. Modern Methods of Plants Analysis 7, 67–162.

Hung, C.C., Wong, G., Liu, K.K., Shiah, F.K., Gong, G.C., 2000. The effects of light and nitrate levels on the relationship between nitrate reductase activity and 15NO3 - uptake: Field observations in the East China Sea. Limnology and Oceanography 45, 836–848.

Jones, G.J., Morel, F.M., 1988. Plasmalemma redox activity in the diatom thalassiosira: a possible role for nitrate reductase. Plant physiology 87, 143–147.

Loick-Wilde, N., Weber, S.C., Conroy, B.J., Capone, D.G., Coles, V.J., Medeiros, P.M., Steinberg, D.K., Montoya, J.P., 2016. Nitrogen sources and net growth efficiency of zooplankton in three Amazon River plume food webs. Limnology and Oceanography 61, 460–481.

MacIsaac, J.J., Dugdale, R.C., 1969. The kinetics of nitrate and ammonia uptake by natural populations of marine phytoplankton. Deep Sea Research 16, 45–57.

MacIsaac, J.J., Dugdale, R.C., 1972. Interactions of light and inorganic nitrogen in controlling nitrogen uptake in the sea. Deep-Sea Research and Oceanographic Abstracts 19, 209–232.

MacIsaac, J.J., Dugdale, R.C., Barber, R.T., Blasco, D., Packard, T.T., 1985. Primary production cycle in an upwelling center. Deep-Sea Research 32, 503–529.

Martinez, R., Packard, T.T., Blasco, D., 1987. Light effects and diel variations of nitrate reductase activity in phytoplankton from the northwest Africa upwelling region. Deep Sea Research 34, 741–753.

Minas, H.J., Coste, J.B., Minas, M., Raimbault, P., 1990. Conditions hydrologiques, chimiques et production primaire dans les upwellings du Perou et des iles Galapagos, en regime d'hiver austral (campagne Paciprod). Oceanologica Acta 10, 383–390.

Packard, T., Blasco, D., MacIsaac, J., Dugdale, R., 1971. Variations of nitrate reductase in marine phytoplankton. Investigaciones Pesqueras 35, 209–219.

Packard, T.T., 1973. The light dependence of nitrate reductase in marine phytoplankton. Limnology and Oceanography 18, 466–469.

Packard, T.T., Blasco, D., 1974. Nitrate reductase activity in upwelling regions. 2. Ammonia and Light dependence. Tethys , 269–280.

Packard, T.T., Blasco, D., Estrada, M., 2004. Modeling physiological processes in plankton on enzyme kinetic principles. Scientia Marina 68, 49–56.

Packard, T.T., Dugdale, R.C., Goering, J.J., Barber, R.T., 1978. Nitrate reductase activity in the subsurface waters of the Peru Current. Journal of Marine Research 36, 59–76.

Packard, T.T., Jones, V., 1976. Biochemistry and ecology of the Peru Current: The JASON expedition to the Peru upwelling system, September 1976, CUEA. Technical Report, 46. Technical Report. Bigelow Laboratory for Ocean Sciences.

Packard, T.T., Osma, N., Fernández-Urruzola, I., Codispoti, L.A., Christensen, J.P., Gómez, M., 2015. Peruvian upwelling plankton respiration: Calculations of carbon flux, nutrient retention efficiency, and heterotrophic energy production. Biogeosciences 12, 2641–2654.

Pickett, M.H., Paduan, J.D., 2003. Ekman transport and pumping in the California Current based on the U.S. Navy's high-resolution atmospheric model (COAMPS). Journal of Geophysical Research 108, 1–10.

Rojas de Mendiola, B., 1976. Phytoplankton analysis of the station samples: The JASON expedition to the Peru upwelling system, September 1976, CUEA. Technical Report, 46. Technical Report. Bigelow Laboratory for Ocean Sciences.

Santoso, A., McGregor, S., Jin, F.F., Cai, W., England, M.H., An, S.I., McPhaden, M.J., Guilyardi, E., 2014. Late-twentieth-century emergence

of the El Niño propagation asymmetry and future projections. Nature 504, 126–130.

Tischner, R., 2000. Nitrate Uptake and Reduction in Plants. Plant, Cell and Environment 23, 1005–1024.

Tischner, R., Ward, M.R., Huffaker, R.C., 1989. Evidence for a plasma-membrane-bound nitrate reductase involved in nitrate uptake of Chlorella sorokiniana. Planta 1, 19–24.

Wooster, W.S., 1961. Yearly Changes in the Peru Current. Limnology and Oceanography , 222–226.

Young, E.B., Dring, M.J., Savidge, G., Birkett, D.A., Berges, J.A., 2007. Seasonal variations in nitrate reductase activity and internal N pools in intertidal brown algae are correlated with ambient nitrate concentrations. Plant, Cell and Environment 30, 764–774.

7. Figures and Tables

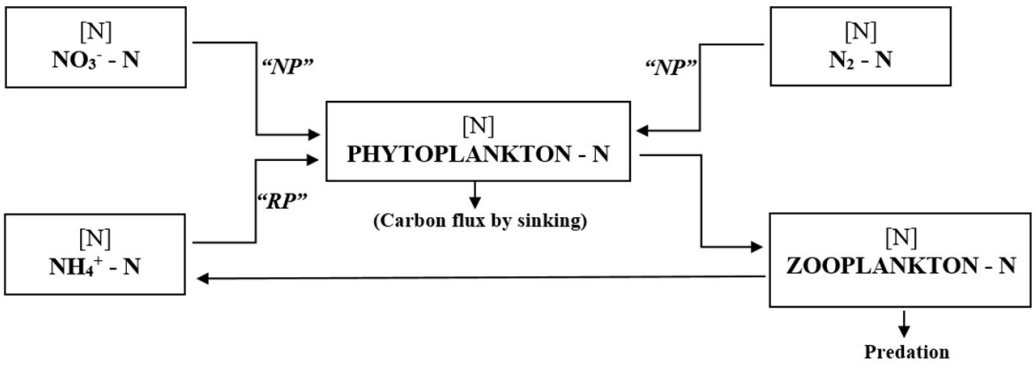

Figure 1: Simplified model of the circulation of inorganic nitrogen (N) through the euphotic zone ecosystem. [N] represent the concentration of nitrogen in each fraction. "NP" and "RP" represent the "New Production" and "Regenerated Production" respectively, driven by the different sources of nitrogen in the system (modified from Dugdale and Goering (1967)).

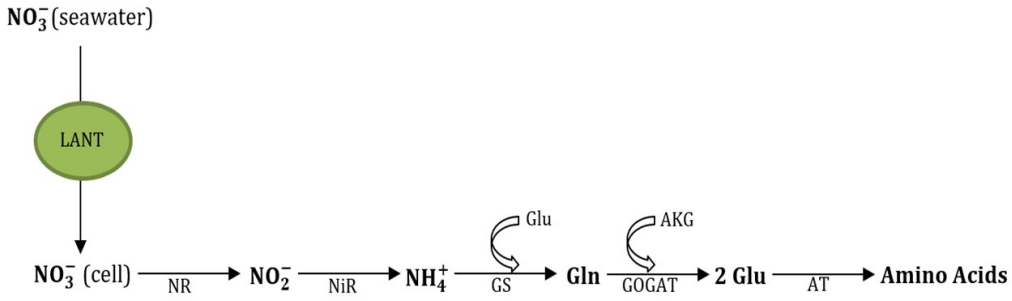

Figure 2: Simplified model of the metabolic route for the NO_3^- conversion into protein. The different enzymes that catalyze the process shown above, along with other key molecules, are: Low Affinity Nitrate Transporters (LAT), Nitrate Reductase (NR), Nitrite Reductase (NiR), Glutamate (Glu), Glutamine Synthetase (GS), Alpha-KetoGlutarate (AKG), Glutamate Synthase (GOGAT) and AminoTransferase (AT). Nitrate Reductase controls the biochemical reaction (modified from Packard et al. (1971) and Glibert et al. (2015)).

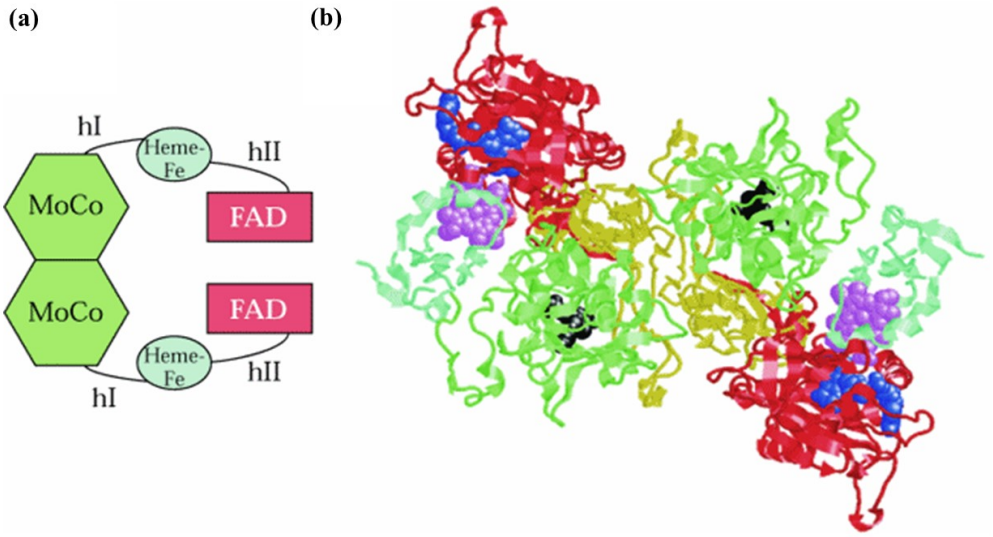

Figure 3: (a) Functional domains of the enzyme nitrate reductase, Flavin (FAD) domain, heme (Fe) domain and molybdenum cofactor (MoCo) domain. (b) Ribbon model of the enzyme nitrate reductase. The NO_3^- reduction starts with e^- transport from NAD(P)H to the flavin domain, passing through heme domain onto NO_3^- via the molybdenum cofactor, to transform nitrate into NO_2^- (taken from Plant Biochemistry, lecture twenty-three: Nitrogen metabolism - nitrate reduction, ammonia assimilation).

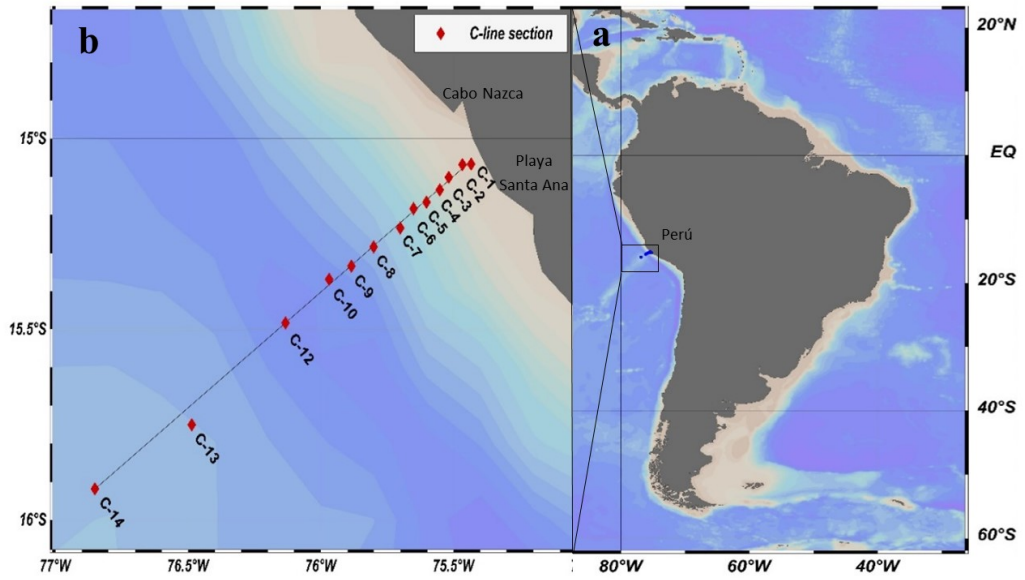

Figure 4: (a) Location of the site of study, in the Peruvian coast at 15°S. (b) C-line section orthogonal to the Peruvian coast at 15°S.

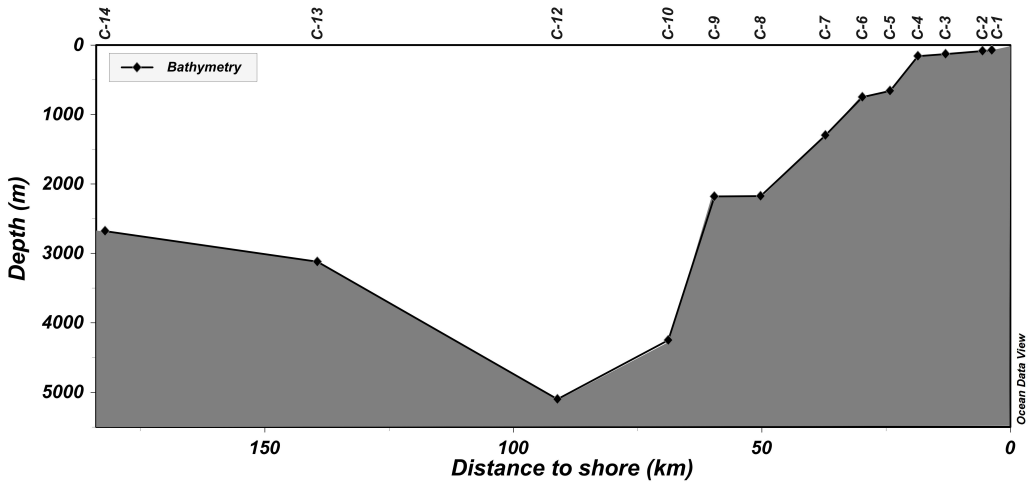

Figure 5: CUEA C-line through the Peru upwelling and Trench at 15°S. Peru coast on the right. The closest C-line position, C-1, was 2.7 km from the coast. C-14 was 185.2 km from the coast, located west of the Peru-Chile trench.

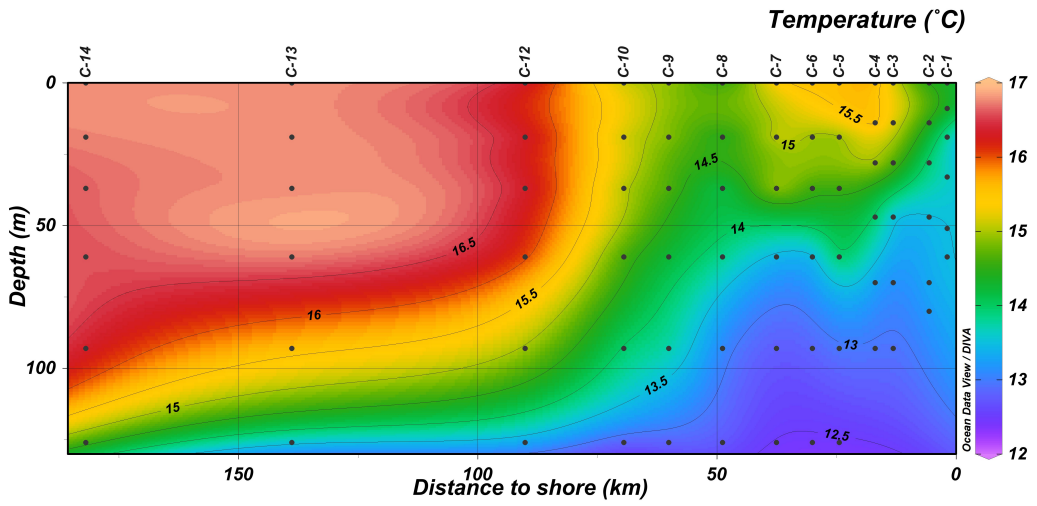

(a) Temperature

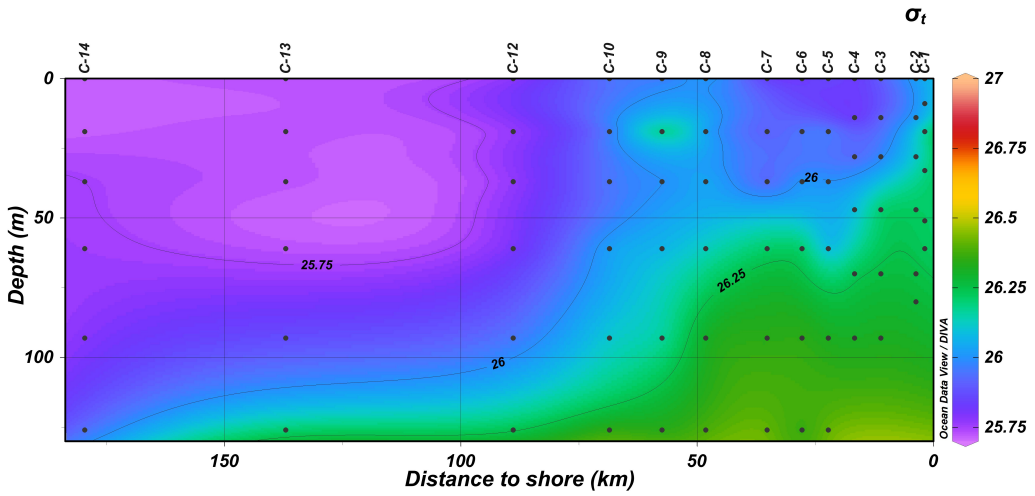

(b) σ_t

Figure 6: Temperature (°C) and density (σ_t) of the column water along the C-line. 10^{th} September, 1976.

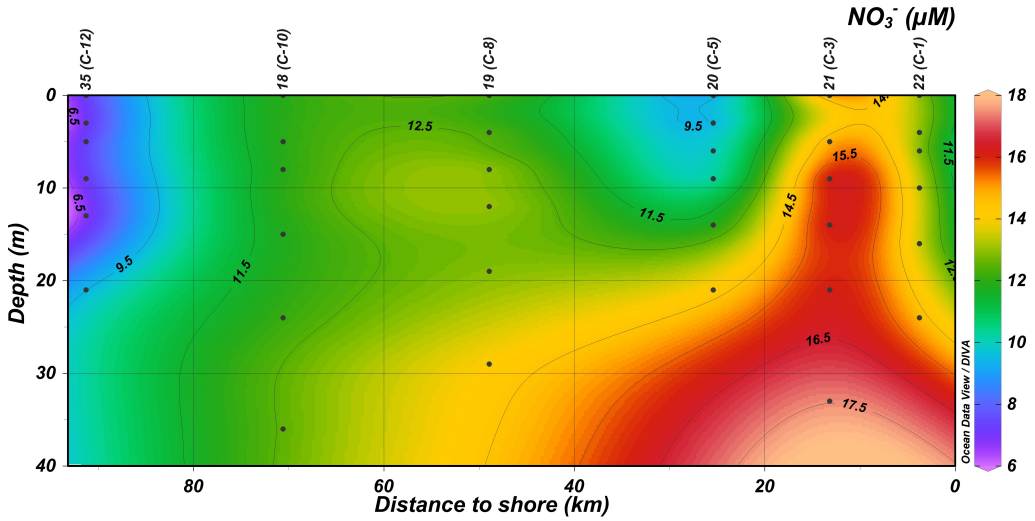

(a) NO_3^-

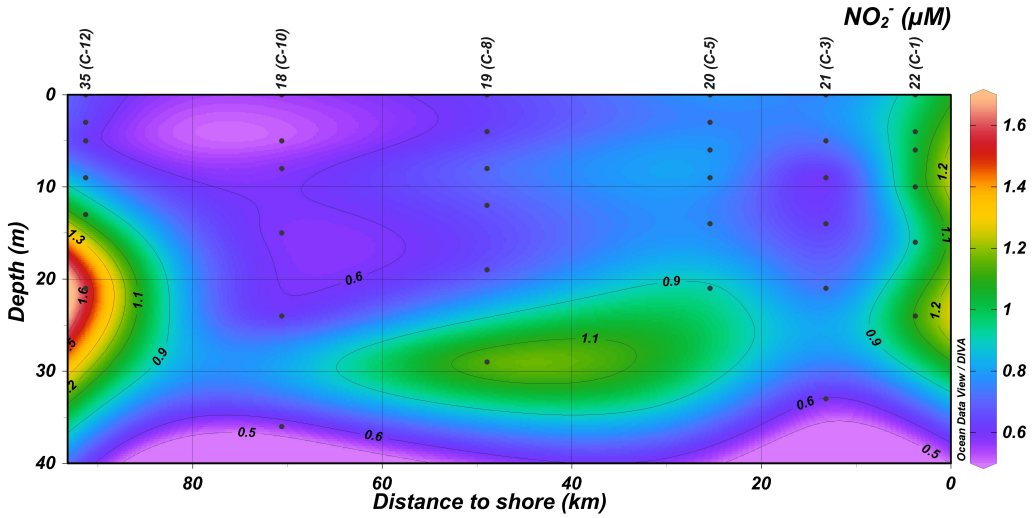

(b) NO_2^-

Figure 7: (a) NO_3^- and (b) NO_2^- sections along the C-line from C-1 to C-12, respectively. Both sections represent the upwelling from 16th to 22th September 1976.

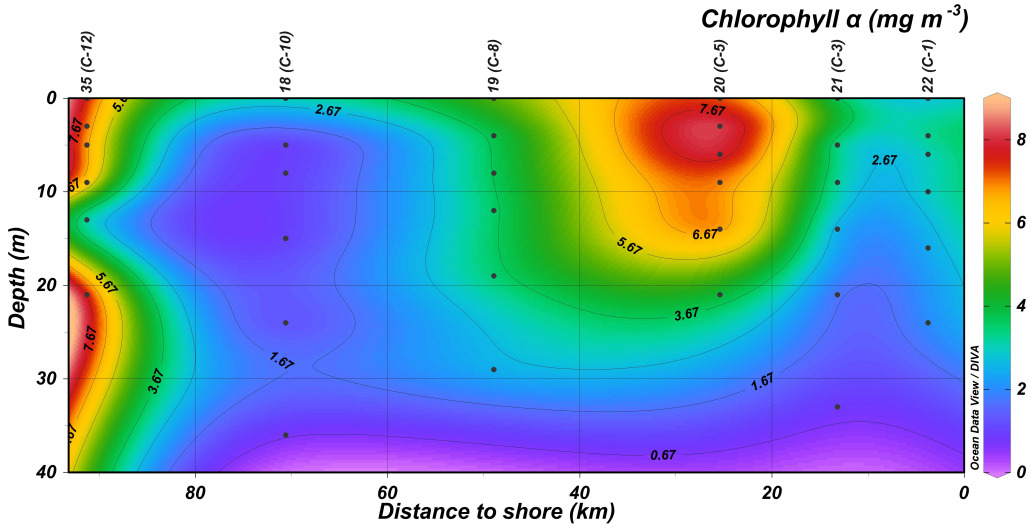

(a) Chlorophyll α

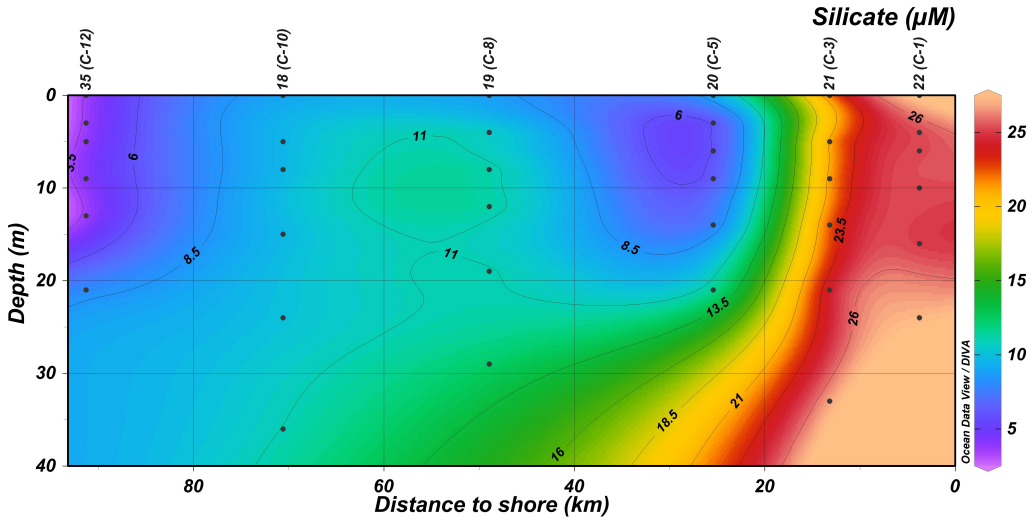

(b) Silicate

Figure 8: (a) Chlorophyll α distribution in the column water along the C-line from C-1 to C-12. (b) Silicate distribution in the water column along the C-line from C-1 to C-12. The values represent the upwelling from 16$^{\text{th}}$ to 22$^{\text{th}}$ September 1976.

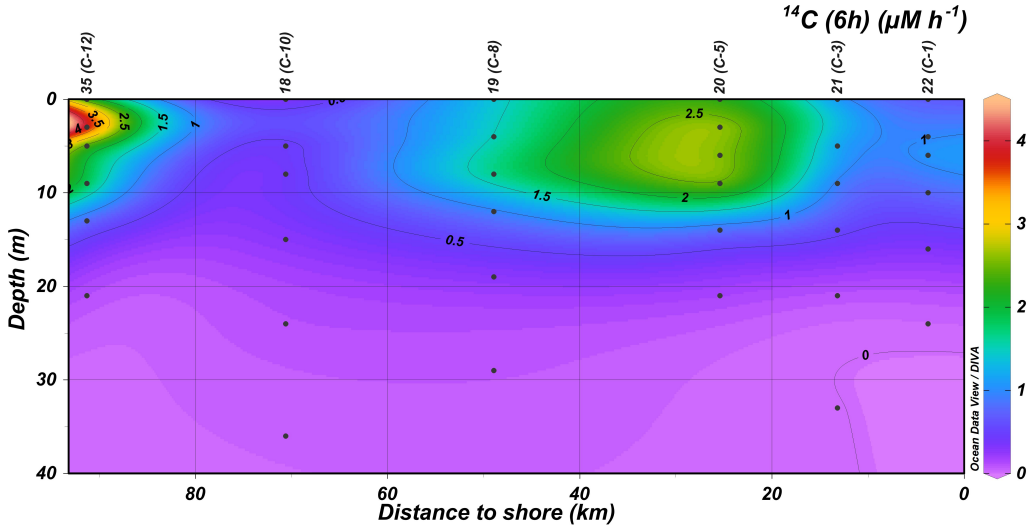

(a) ^{14}C (6h)

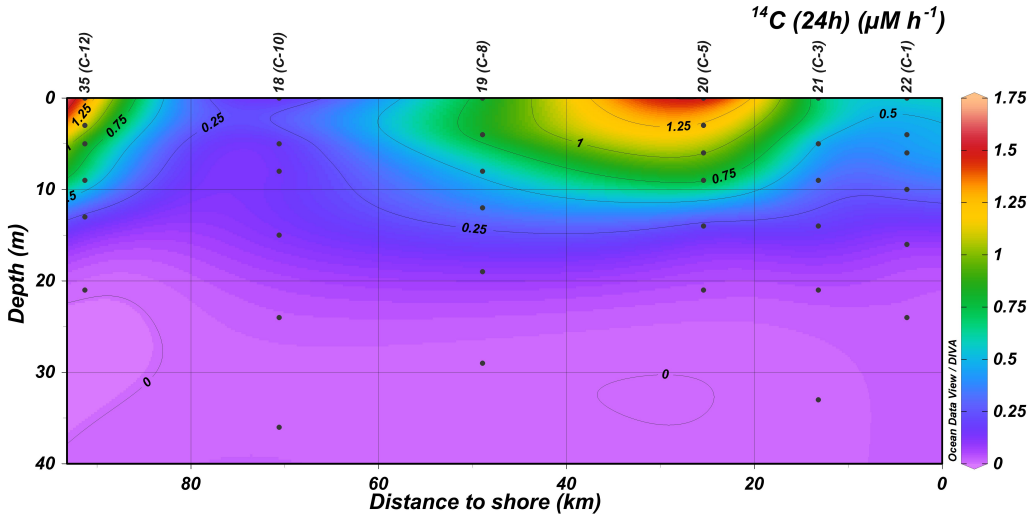

(b) ^{14}C (24h)

Figure 9: ^{14}C Productivity along the C-line from C-1 to C-12 as calculated from: (a) 6-h and (b) 24-h deck-incubated bottled phytoplankton. Both measurements correspond to the upwelling system of Peru coast from 16$^{\text{th}}$ to 22$^{\text{th}}$ September 1976.

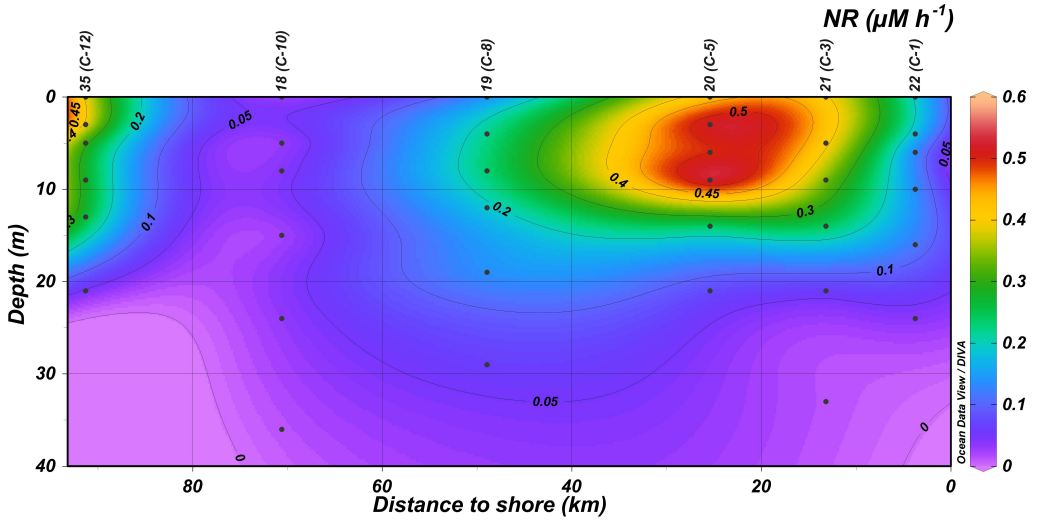

Figure 10: Distribution of the Nitrate Reductase activity expressed in μM of N, in the upwelling system of Peru coast, from 16$^{\text{th}}$ to 22$^{\text{th}}$ September 1976.

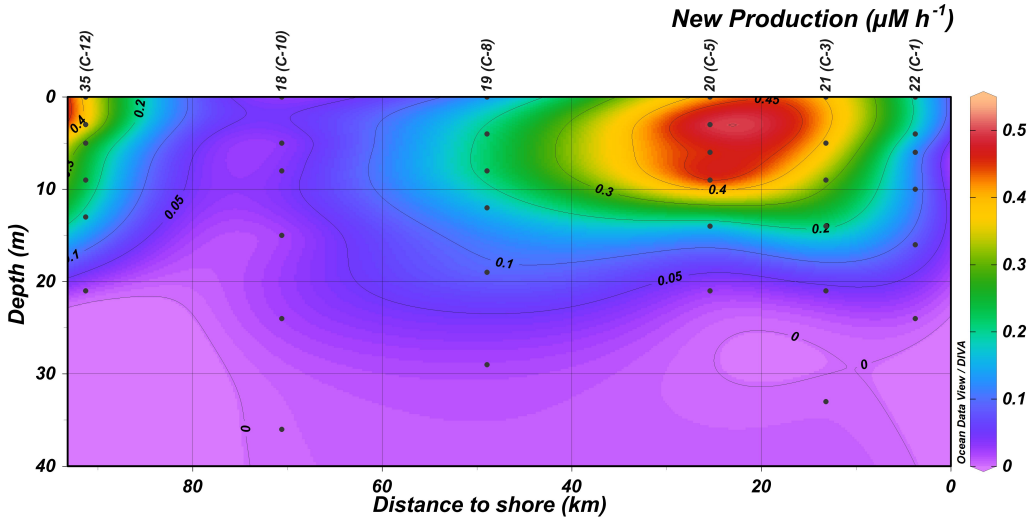

(a) New Production in terms of nitrogen

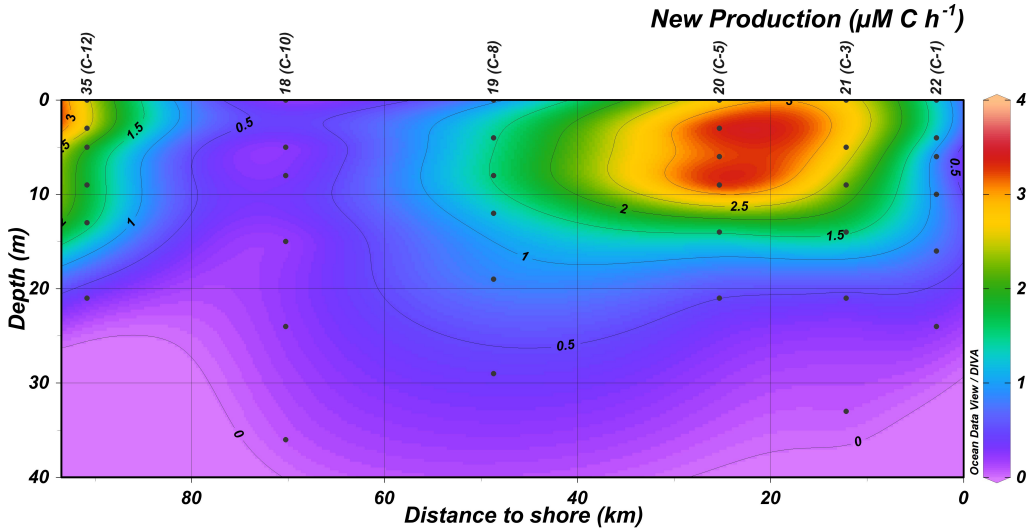

(b) New Production in terms of carbon

Figure 11: New production in terms of: (a) Nitrogen along the C-Line from C-1 to C-12 calculated from NR activity measured in phytoplankton, and (b) Carbon along the C-Line from C-1 to C-12 calculated from NR activity measured in phytoplankton. Both measurements correspond to the upwelling system of Peru coast 16$^{\text{th}}$ to 22$^{\text{th}}$ September 1976.

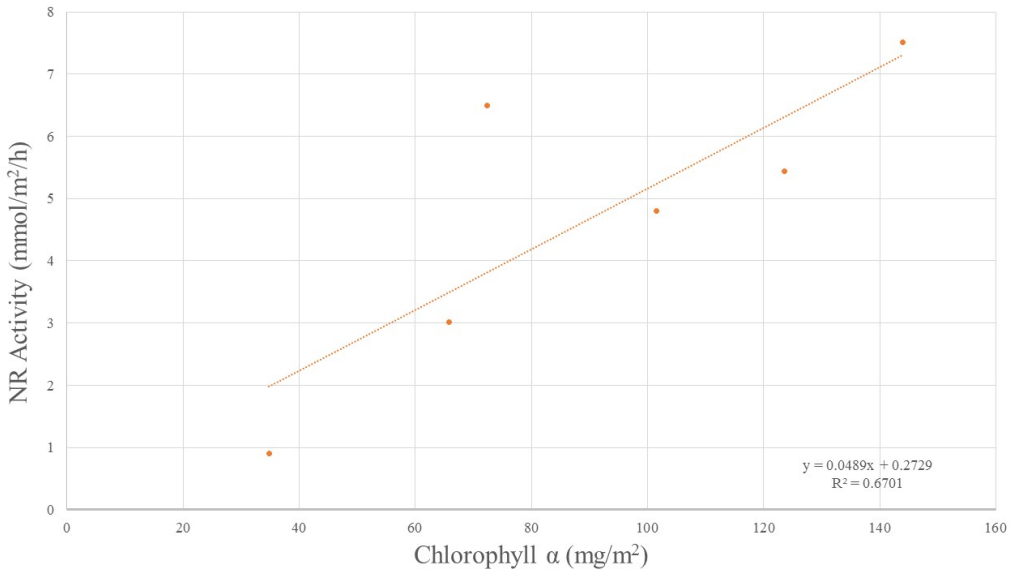

Figure 12: Correlation between integrated values of NR activity and chlorophyll derived from Table 3.

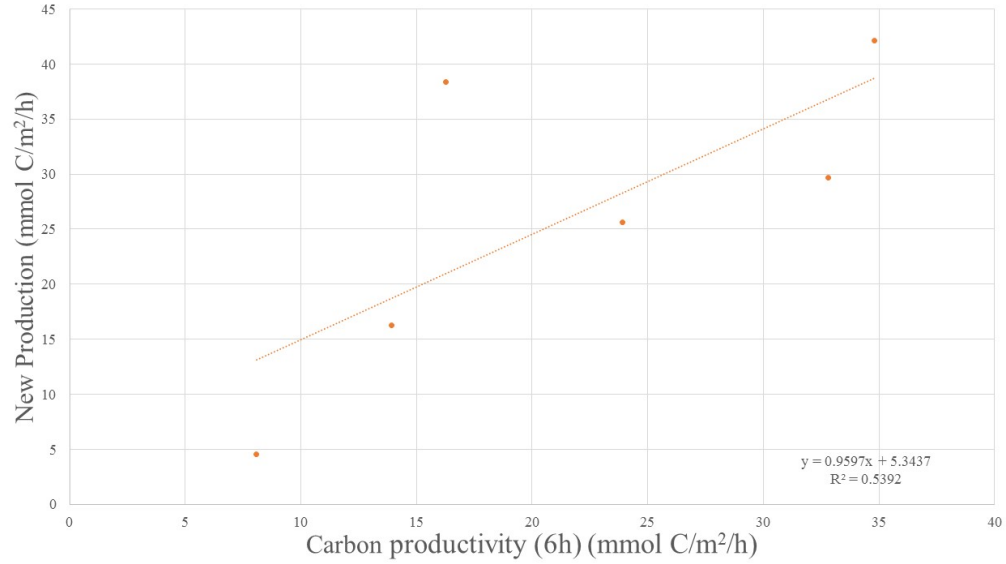

(a) 6 h incubation

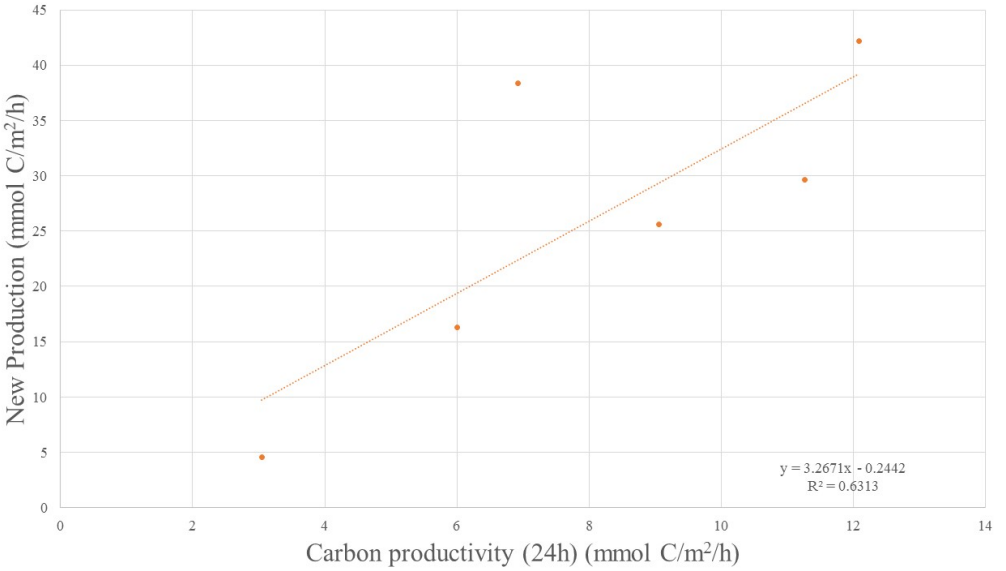

(b) 24 h incubation

Figure 13: Correlation between integrated new production in terms of carbon and integrated carbon productivity as calculated from: (a) 6-h and (b) 24-h deck-incubated bottled phytoplankton.

Table 1: Biochemical characteristics of Peruvian upwelling along the C-line during JASON-76 R/V Eastward cruise no. E-5H-67 in 10^{th} September 1976. In column 1 are the station number, time of sampling and day on September 1976. All data have been converted to L basis from the original data. Coordinates and oceanographic characteristic in these same stations are present in Table 1 of Packard et al. (2015). Original data are present in CUEA data reports (Packard and Jones, 1976).

CUEA	**Depth**	**NR**	**Chl.**	**Prot.**	**NO_3^-**	**NO_2^-**	**SiO_4^{4-}**	**PO_4^{3-}**	**^{14}C(24h)**	**^{14}C(6h)**
C-line section	(m)	(μM h^{-1})	(μg L^{-1})	(μM)	(μM)	(μM)	(μM)	(μM)	(μM C h^{-1})	(μM C h^{-1})
C10 (18)	0	0.02892	1.06	3.61	11.92	0.52	9.7	0.94	1.64	3.41
Day 16	5	0.02313	0.9	3.05	11.93	0.51	9.6	0.93	1.73	4.63
13:43	8	0.03709	1	2.7	11.82	0.58	9.6	0.91	1.73	4.3
	15	0.01552	0.96	2.47	11.82	0.58	9.7	0.91	1.51	3.64
	24	0.03229	1.13	4.81	12.10	0.58	10.1	0.94	0.37	1.51
	36	0.01453	0.67	3.82	12.54	0.54	11	0.98	0.16	0.59
C8 (19)	0	0.13923	4.11	8.41	12.42	0.82	11.3	1.17	9.65	17.2
Day 17	4	0.22473	3.8	8.68	12.56	0.64	11	1.17	10.15	18
13:30	8	0.2378	3.75	8.27	13.20	0.72	11.5	1.19	6.47	21.18
	12	0.1926	3.55	8.47	13.24	0.68	11.6	1.18	4.5	11.2
	19	0.15081	3.59	6.42	12.93	0.67	11.3	1.16	1.2	3.36
	29	0.06557	2.62	66.84	14.15	1.21	12.5	1.25	0.07	1.09
C5 (20)	0	0.42414	6.96	17.91	9.21	0.79	5.6	0.93	18.24	26.81
Day 18	3	0.53399	8.34	18.99	9.24	0.76	5.6	0.93	14.91	32.45
13:25	6	0.4779	8.08	21.62	9.76	0.8	5.7	0.94	12.18	30.64
	9	0.56735	6.93	20.38	9.79	0.81	6	0.97	9.64	31.99
	14	0.21918	7.1	-	11.59	0.77	7.3	1.03	2.22	8.77
	21	0.07376	3.99	5.18	14.15	0.93	1	1.16	0.53	2.14

Continued on next page

C-line section	Depth	NR	Chl.	Prot.	NO_3^-	NO_2^-	SiO_4^{4-}	PO_4^{3-}	^{14}C(24h)	^{14}C(6h)
C3 (21)	0	0.4042	3.67	6.43	15.24	0.76	22.2	1.44	8.08	12.97
Day 19	5	0.40927	3.14	5.66	15.19	0.73	21.8	1.42	5.54	13.57
13:27	9	0.33345	3.15	5.39	16.62	0.58	21.7	1.47	3.92	10.66
	14	0.25155	2.36	4.91	16.45	0.63	22.9	1.51	2.4	6.88
	21	0.05584	1.64	2.98	16.28	0.72	24.8	1.51	0.56	1.3
	33	0.01605	0.86	1.01	17.5	0.58	26.9	1.63	0.11	0.05
C1 (22)	0	0.19273	3.06	7.07	12.93	1	25	1.51	6.84	8.46
Day 20	4	0.18613	3.37	8.73	13.03	1.01	25.2	1.51	5.44	11.66
13:28	6	0.12456	3.01	9.36	12.76	1.03	25.3	1.5	5.2	13.28
	10	0.13893	3.01	6.66	13.37	1.05	25.3	1.53	3.62	9.28
	16	0.12085	2.47	6.21	13.4	0.92	24.9	1.53	0.98	3.88
	24	0.03896	2.07	-	14.73	1.13	27.2	1.64	0.37	0.47
C12 (35)	0	0.39047	7.47	-	7.36	0.68	4	0.88	16.64	25.91
Day 22	3	0.40368	7.09	-	6.99	0.65	3.7	0.84	13.51	50.34
13:28	5	0.29856	6.72	-	7.42	0.62	3.9	0.86	10.12	25.06
	9	0.28159	6.51	-	7.29	0.79	4.3	0.84	7.74	23.66
	13	0.27529	2.87	-	6.65	1.03	3.5	0.85	2.47	8.88
	21	0.04239	7.8	-	9.56	1.6	8.2	0.97	0.08	1.51

Table 2: Calculations of new production (NP) in terms of nitrogen and carbon. NP in terms of nitrogen is based on Eq. 4 and on the light and nitrate reductase (NR) activity across the C-line for the cross-shelf section on 16^{th}-22^{th} September 1976. NP in terms of carbon was obtained by multiplying NP (in terms of nitrogen) by 6.6, the C:N Redfield ratio (Geider and La Roche, 2002).

CUEA	**Depth**	**hυ**	**hυ**	**NR**	**NO_3^-**	**New production**	**New production**
C-line section	(m)	(ly min^{-1})	(%I_0)	(μM h^{-1})	(μM)	(μM N h^{-1})	(μM C h^{-1})
C10 (18)	0	35.1	100	0.03	11.92	0.03	0.19
Day 16	5	17.55	50	0.02	11.93	0.02	0.15
13:43	8	10.53	30	0.04	11.82	0.04	0.24
	15	5.265	15	0.02	11.82	0.02	0.10
	24	1.755	5	0.03	12.10	0.03	0.21
	36	0.351	1	0.01	12.54	0.004	0.03
C8 (19)	0	54.8	100	0.14	12.42	0.14	0.92
Day 17	4	27.4	50	0.22	12.56	0.22	1.48
13:30	8	16.44	30	0.24	13.20	0.24	1.56
	12	8.22	15	0.19	13.24	0.19	1.26
	19	2.74	5	0.15	12.93	0.15	0.97
	29	0.548	1	0.07	14.15	0.06	0.41
C5 (20)	0	73.8	100	0.42	9.21	0.42	2.79
Day 18	3	36.9	50	0.53	9.24	0.51	3.49
13:25	6	22.14	30	0.48	9.76	0.47	3.10
	9	11.07	15	0.57	9.79	0.55	3.61
	14	3.69	5	0.22	11.59	0.21	1.39
	21	0.738	1	0.07	14.15	0.07	0.45
C3 (21)	0	49.6	100	0.40	15.24	0.40	2.66
Day 19	5	24.8	50	0.41	15.19	0.41	2.68
13:27	9	14.88	30	0.33	16.62	0.33	2.18
	14	7.44	15	0.25	16.45	0.25	1.63
	21	2.48	5	0.06	16.28	0.06	0.36
	33	0.496	1	0.02	17.50	0.02	0.10
C1 (22)	0	72	100	0.19	12.93	0.19	1.27
Day 20	4	36	50	0.19	13.03	0.19	1.22
13:28	6	21.6	30	0.12	12.76	0.12	0.82
	10	10.8	15	0.14	13.37	0.14	0.91

Continued on next page

C-line section	Depth	hv	hv	NR	NO_3^-	New production	New production
	16	3.6	5	0.12	13.40	0.12	0.78
	24	0.72	1	0.04	14.73	0.04	0.25
C12 (35)	0	42.1	100	0.39	7.36	0.39	2.57
Day 22	3	21.5	50	0.40	6.99	0.40	2.64
13:28	5	12.63	30	0.30	7.42	0.30	1.95
	9	6.32	15	0.28	7.29	0.28	1.82
	13	2.11	5	0.28	6.65	0.26	1.72
	21	0.42	1	0.04	9.56	0.04	0.27

Table 3: Integrated values over the euphotic zone (Ez) for the cross-shelf section on 16^{th}-22^{th} September 1976 during JASON-76 R/V Eastward cruise no. E-5H-67 in September 1976, and integrated new production, in terms of N, calculated from our model. Coordinates and oceanographic characteristic in these same stations are present in Table 1 of Packard et al. (2015). Original data are present in CUEA data reports (Packard and Jones, 1976). New production in carbon was calculated using the C:N Redfield Ratio of 6.6 (Geider and La Roche, 2002). The average values per m^3 for the Ez properties (above) can be calculated, dividing by Ez.

CUEA C-Line	**Ez**	**NR**	**Chl. a**	**Protein**	**NO_3^-**	**NO_2^-**	**SiO_4^{4-}**	**PO_4^{3-}**	**^{14}C(24h)**	**^{14}C(6h)**	**New Prod.**
	(m)	(mmol m^{-2} h^{-1})	(mg m^{-2})	(mmol m^{-2})	(mmol m^{-2})	(mmol m^{-2})	(mmol m^{-2})	(mmol m^{-2})	(mmol m^{-2} C h^{-1})	(mmol m^{-2} C h^{-1})	(mmol m^{-2} N h^{-1})
C10 (18) Day 16	36	0.9	34.82	127.91	433.47	20.21	360.3	33.65	3.05	8.1	0.69
C8 (19) Day 17	29	4.8	101.56	219.98	429.98	22.7	334.95	34.38	12.42	23.9	3.88
C5 (20) Day 18	21	7.51	143.99	179.27	229.04	16.98	149.3	21.13	13.53	34.8	6.39
C3 (21) Day 19	33	6.49	72.38	129.63	539.61	21.9	785.65	49.79	6.92	16.28	5.81
C1 (22) Day 20	24	3	65.88	120.34	322.8	24.33	611.1	36.97	6	13.93	2.47
C12 (35) Day 22	21	5.44	123.55	-	158.1	20.25	97.95	18.34	11.27	32.82	4.49